Copyright © 2002 IFAC
15th Triennial World Congress, Barcelona, Spain

EFFICIENT MODELS FOR FLEXIBLE MANIPULATORS WITH MOTORS AT THE JOINTS

L. Bascetta [*], **F. Bernasconi** [**], **A. Locatelli** [*] and **P. Rocco** [*]

[*] *Politecnico di Milano, Dipartimento di Elettronica e Informazione, Piazza Leonardo da Vinci, 32, 20133, Milano, Italy {bascetta, locatelli, rocco}@elet.polimi.it*
[**] *SIAE Microelettronica S.p.a., Via Michelangelo, 21, 20093, Cologno Monzese (Milano), Italy*

Abstract A computationally efficient recursive algorithm to model flexible manipulators is described in this paper. The dynamic effects, including gyroscopic terms, of the motors at the joints are fully taken into account. Symbolic simplification is used in a newly developed package (FLEXROB), whose performance in detailed reproduction of the dynamic effects due to the interplay between the motors and the flexible links is assessed through simulation.

Keywords: Flexible arms, Dynamic modelling, Simulation, Efficient algorithms, Model approximation.

1. INTRODUCTION

Lightweight flexible manipulators are used today in a variety of applications, ranging from the traditional space robotics field to less known tasks, like exploration of hazardous environments or nuclear waste retrieval. Use of lightweight structures in industrial applications is also an interesting alternative to the use of bulky and massive traditional industrial robots.
Advances in dexterity and power consumption are expected. Reduced masses and extended workspaces however enhance the effects of the flexibility of the materials, making an accurate modelling of the system crucial, both for simulation and for control purposes. Besides accuracy in reproducing the dynamic effects due to the flexibility, the model is expected to be efficient, so as to lend itself to intensive computation, as required by realtime simulation or model based control. In this respect, recursive algorithms, where the chain structure of a serial manipulator is fully exploited, have long been known to be superior to algorithms derived from the modelling of the manipulator as a whole mechanical system.
The modelling task is even harder if the role of the actuators is considered in a rigorous way, as it will be shown in the present paper. Consider that the masses of a flexible link and of its actuator (e.g. an electrical motor at the joint) could be comparable: neglecting or oversimplifying the dynamic effects of the motors could then yield severe errors in the simulation of the system.

In his pioneering work (Book, 1984) Book derived the model of a serial flexible manipulator from Lagrange's equations in a recursive form. The formulation, improved in (Cetinkunt and Book, 1987) with symbolic computation, suffers however from the intrinsic computational inefficiency of the Euler-Lagrange equations of a system of bodies. In (Hughes and Sincarsin, 1989) a model of a flexible manipulator based on Newton-Euler and finite element techniques is proposed. Other authors (Singh *et al.*, 1984) derived the model using D'Alembert's principle applying global balances from virtual power evaluation and Kane's kinematic modelling (Kane and Levinson, 1980). In (Boyer and Coiffet, 1996) each link is cleverly considered as a free elastic body and dynamic equilibria are derived from virtual power computation. This allows to obtain in a remarkably linear way the formulation of the dynamic model of the link. Then, assembling the models of the links in a similar way as in the well known Newton-Euler formulation for rigid robotics

yields an efficient recursive algorithm for computing the dynamics of the whole manipulator.

The first part of the present paper is an extension of (Boyer and Coiffet, 1996): the same methodology is in fact used to derive first the model of a flexible body coupled to a rigid rotary actuator and then to formulate the dynamic model of a whole serial link flexible manipulator with motors at the joints. The study is restricted to low joint speeds, thus neglecting the second order effects of elastic deformations, and linear elastic kinematics, as in (Padilla and Flottow, 1992) and (Kane *et al.*, 1987).
As the model becomes considerably more involved than the motor-less model, computer algebra is needed to simplify it, based on the actual configuration of the manipulator and its physical parameters. A package (FLEXROB) has then been developed under the commercial symbolic environment *Maple* 6©, making use of its advanced object-oriented features. Remarkably, the package produces an efficient dynamic model in the form of an S-function, ready to be numerically integrated in *Simulink*©.
Simulation results are finally presented, focusing on the importance of accurate modelling of the dynamic effects induced by the presence of the motors at the joints with respect to approximated solutions. In particular the straightforward solution where only the inertial effects of the rotors around their own axes is considered, thus neglecting gyroscopic and mass effects (which corresponds to add a constant diagonal matrix to the inertia matrix of the flexible manipulator) is shown to produce significant errors, compared to the complete model.

The paper is structured as follows. The principle of virtual powers, used to derive the dynamic model, is described in Section 2.1, and the modelling of a flexible link with a motor is considered. The joint equilibrium equation and a kinematic recursive algorithm that relates each link of the chain to the next one are introduced in Section 2.2, to complete the dynamic model of a flexible manipulator with motors. Section 3 considers a simulation example on a prototype flexible manipulator and analyzes the differences between the results produced by the complete model and a simplified one, in which motors are modelled as simple rotating inertias. Conclusions are given in Section 4.

2. DYNAMIC MODEL

2.1 *Model of a flexible link with a motor*

A flexible link can be considered as a free elastic body S, described by the current configuration $\Sigma(t)$ at the current time t, and its motion can be expressed as a superimposition of two contributions: the rigid motion, described in an Eulerian formalism, and the elastic one, which is better described using a Lagrangian formalism, since the description of the deformation state requires the adoption of a reference configuration.
The link velocity field is defined as the following screw [1]

$$\begin{aligned}\underline{\mathbf{D}}^*_{lnk}(M) &= \underline{\mathbf{D}}^*_{lnk_r}(M) + \underline{\mathbf{D}}^*_{lnk_e}(M) \\ &= \left\{ \begin{array}{c} \underline{\mathbf{V}}^*_r + \underline{\omega}^*_r \times \underline{\mathbf{r}}(M) \\ \underline{\omega}^*_r \end{array} \right\} + \left\{ \begin{array}{c} \underline{\mathbf{V}}^*_e(M) \\ \underline{\omega}^*_e(M) \end{array} \right\}\end{aligned}$$

where $\underline{\mathbf{r}}(M)$ denotes the position vector $\underline{\mathbf{O_0M}}$, and the point O_0 is the reference point which belongs to the current configuration $\Sigma_0(t)$, at the current time t, of the reference body S_0 associated to the body S.
The two velocities $\underline{\mathbf{V}}_r$ and $\underline{\omega}_r$, which form a set of Eulerian kinematic variables, describe the rigid component of the motion. Instead the vector fields $\underline{\omega}_e$ and $\underline{\mathbf{V}}_e$ are the elastic angular and linear velocity fields respectively. These Eulerian elastic fields are approximated by a finite set of independent Lagrangian velocities $\dot{q}_{e1}, \dot{q}_{e2}, \ldots \dot{q}_{eN}$ using the Rayleigh-Ritz decomposition (Meirovitch, 1967)

$$\underline{\mathbf{D}}^*_{lnk}(M) = \left\{ \begin{array}{c} \underline{\mathbf{V}}^*_r + \underline{\omega}^*_r \times \underline{\mathbf{r}}(M) \\ \underline{\omega}^*_r \end{array} \right\} + \sum_{k=1}^{N} \left\{ \begin{array}{c} \underline{\Phi}_{dk}(M_0) \\ \underline{\Phi}_{rk}(M_0) \end{array} \right\} \cdot \dot{q}^*_{ek}$$

where $\underline{\Phi}_{dk}$ and $\underline{\Phi}_{rk}$ are the k^{th} displacement and rotation shape functions respectively, N is the number of shape functions and the point M_0 ($\in \Sigma_0(t)$) is the correspondent of the point M ($\in \Sigma(t)$) on the reference body.
With the same notation, considering the motor as a rigid body whose center of gravity is located at a point $M_{mot} \in \Sigma(t)$, the rotor velocity field can be defined as the following screw

$$\underline{\mathbf{D}}^*_{mot}(M_{mot}) = \left\{ \begin{array}{c} \underline{\mathbf{V}}^*_r + \underline{\omega}^*_r \times \underline{\mathbf{r}}(M_{mot}) \\ \underline{\omega}^*_r + k_r \dot{q}^*_m \underline{\mathbf{z}}_m \end{array} \right\} + \sum_{k=1}^{N} \left\{ \begin{array}{c} \underline{\Phi}_{dk}(M_{mot_0}) \\ \underline{\Phi}_{rk}(M_{mot_0}) \end{array} \right\} \cdot \dot{q}^*_{ek}$$

where k_r is the transmission ratio, $\dot{q}_m$ is the velocity of the rotor and $\underline{\mathbf{z}}_m$ a vector along its axis.

To derive the dynamic equilibria the principle of virtual powers (or D'Alembert's principle) will be used, since this principle includes both Eulerian and Lagrangian approaches.
The balance equation of virtual powers can be written as follows

$$P^*_{acc\ lnk,g} + P^*_{acc\ mot,g} = P^*_{int} + P^*_{ext,g}$$ [2]

where $P^*_{acc\ lnk,g}$, $P^*_{acc\ mot,g}$ are the virtual powers of acceleration fields of the link, inclusive of stator, and of the rotor, respectively, and P^*_{int}, $P^*_{ext,g}$ are the virtual powers of internal cohesion forces and external forces acting on S, respectively.

The virtual power of the acceleration field applied on the body is the integral on Σ_0 of the internal product

[1] We use "$*$" to distinguish the virtual fields from their real homologous ones.
[2] The suffix "$_g$" refers to a Galilean frame denoted by R_g

involving the acceleration wrench density and the virtual velocity screw, both evaluated at M

$$P^*_{acc\ lnk,g} = \int_{\Sigma_0} \langle \underline{\mathbf{D}}^*_{lnk}(M), d\underline{\mathbf{T}}_{acc\ lnk}(M) \rangle$$

where the wrench field of acceleration quantities is as follows

$$d\underline{\mathbf{T}}_{acc\ lnk}(M) = dm \left\{ \begin{array}{c} \underline{\gamma}_{lnk}(M) \\ \underline{\mathbf{0}} \end{array} \right\}$$

and $\underline{\gamma}_{lnk}(M)$ is the acceleration field deduced from the differentiation of the linear velocity field (the momentum is the null vector since the particle of mass dm has no spin, having no volume).

The virtual power of the acceleration field applied to the motor is

$$P^*_{acc\ mot,g} = \langle \underline{\mathbf{D}}^*_{mot}, \underline{\mathbf{T}}_{acc\ mot} \rangle$$

where the wrench field of acceleration quantities is

$$\underline{\mathbf{T}}_{acc\ mot} = \left\{ \begin{array}{c} m_m \underline{\gamma}_{mot} \\ I_m \underline{\mathbf{h}}_{mot} \end{array} \right\}$$

and m_m, I_m are the rotor mass and moment of inertia, respectively; $\underline{\gamma}_{mot}$, $\underline{\mathbf{h}}_{mot}$ are deduced from the differentiation of the linear and angular velocity field.

The following external forces act onto each isolated link: the gravity field; the constraint forces and torques transmitted by the previous and the following joints at geometric points, denoted by A and A' respectively; the control forces and torques also applied in A and A'.

The virtual power of the gravity field is written as

$$P^*_{wgt,g} = \int_{\Sigma(t)} \langle \underline{\mathbf{D}}^*_{lnk}(M), d\underline{\mathbf{T}}_g(M) \rangle$$

where the gravity force wrench is

$$d\underline{\mathbf{T}}_g(M) = dm \left\{ \begin{array}{c} \underline{\mathbf{g}} \\ \underline{\mathbf{0}} \end{array} \right\}$$

and $\underline{\mathbf{g}}$ is the acceleration gravity field.
The constraint and control wrenches acting onto an isolated link can be written as

$$\underline{\mathbf{T}}_C(A) = \left\{ \begin{array}{c} \underline{\mathbf{F}} \\ \underline{\mathbf{C}} \end{array} \right\} \quad \underline{\mathbf{T}}_C(A') = \left\{ \begin{array}{c} -\underline{\mathbf{F}}' \\ -\underline{\mathbf{C}}' \end{array} \right\}$$

The contribution of these wrenches to the power balance can be written as

$$P^*_{c,g} = \langle \underline{\mathbf{D}}^*_{lnk}(A), \underline{\mathbf{T}}_c(A) \rangle + \langle \underline{\mathbf{D}}^*_{lnk}(A'), \underline{\mathbf{T}}_c(A') \rangle$$

The virtual power of internal forces, if the internal strain energy is expressed as a quadratic form of the generalized elastic coordinates, can be written as

$$P^*_{int}(S) = \sum_{i=1}^{N} \sum_{j=1}^{N} -(k_{ij} q_{ej})\ q^*_{ei}$$

where the k_{ij}'s are generalized stiffnesses.

Including each of the virtual power previously shown in the balance equation leads to the following equality

$$\underline{\mathbf{A}} \cdot \underline{\mathbf{V}}^*_r + \underline{\mathbf{B}} \cdot \underline{\omega}^*_r + \underline{\mathbf{C}} \cdot \dot{q}^*_m \underline{\mathbf{z}}_m + \sum_{i=1}^{N} Q_{ei}\ \dot{q}^*_{ei} = 0$$

where $\underline{\mathbf{A}}$, $\underline{\mathbf{B}}$, $\underline{\mathbf{C}}$ and the Q_{ei}'s are the factors of the virtual kinematic variables.
Since the Eulerian velocities $\underline{\mathbf{V}}^*_r$, $\underline{\omega}^*_r$ and $\dot{q}^*_m$ and the Lagrangian ones $\dot{q}^*_{e1}, \dot{q}^*_{e2}, \ldots \dot{q}^*_{eN}$ are independent, four sets of equilibria can be deduced from this equation (three Eulerian and one Lagrangian)

$$\underline{\mathbf{A}} = \underline{\mathbf{0}} \qquad \underline{\mathbf{B}} = \underline{\mathbf{0}} \qquad \underline{\mathbf{C}} = \underline{\mathbf{0}}$$

$$Q_{e1} = 0, \ldots, Q_{eN} = 0$$

These equilibria take the following interpretations:

- the rigid linear equilibrium, deduced from "$\underline{\mathbf{A}} = \underline{\mathbf{0}}$", that is an extension of the Newton equation
- the rigid angular equilibrium, deduced from "$\underline{\mathbf{B}} = \underline{\mathbf{0}}$", that is an extension of the Euler equation
- the i^{th} elastic equilibrium, deduced from "$Q_{ei} = 0$"

From the equation "$\underline{\mathbf{C}} = \underline{\mathbf{0}}$" the angular equilibrium of the rotor, considered as a free body, can be deduced, that is not of interest in the development of the dynamic model.

Finally all the equilibria can be concatenated in a matricial form, obtaining the dynamic model equation of a single link (see next page). The terms of this equation represent, from left to right, the generalized global inertia matrix, the vector of accelerations, the inertia forces and torques, the generalized stiffness matrix, the gravity forces and torques, the constraint and control forces and torques (see (Boyer and Coiffet, 1996) for the definitions of the inertia parameters).

2.2 *Model of a flexible manipulator with motors*

The complete dynamic model of a flexible manipulator with motors can be written by adding to the dynamic equation of the single link two other relations: the recurrence on velocities and the joint equilibrium equation.

Consider an open chain of n flexible links $S_1, S_2, \ldots S_n$ along with the flexible basis S_0 embedded at the point A_0. The kinematic chain is described by n punctual joints. Each joint introduces at its geometric center A_j one degree of freedom which is either linear or angular and described using the joint Lagrangian variable q_{rj}. In order to derive the constraint equations of the $j+1^{st}$ joint, two consecutive bodies of the chain denoted by S_j and S_{j+1}, connected via the punctual joint in A_{j+1}, can be isolated. The kinematic equation that relates the velocities of these two bodies, i.e. the recurrence on velocities, is the following

$$\begin{pmatrix} \underline{\mathbf{M}}_t & \underline{\mathbf{M}}\hat{\underline{\mathbf{S}}}_t & \underline{\mathbf{MS}}_{de} & \underline{\mathbf{0}} \\ \underline{\mathbf{M}}\hat{\underline{\mathbf{S}}}_t^T & \underline{\mathbf{I}}_t & \underline{\mathbf{MS}}_{re} & \underline{\mathbf{I}}_{rot} \\ \underline{\mathbf{MS}}_{de}^T & \underline{\mathbf{MS}}_{re}^T & \underline{\mathbf{m}}_{ee} & \underline{\mathbf{MS}}_{re_m}^T \end{pmatrix} \begin{Bmatrix} \underline{\gamma}_{linr} \\ \underline{\gamma}_{angr} \\ \ddot{\underline{\mathbf{q}}}_e \\ \ddot{q}_m \underline{\mathbf{z}}_m \end{Bmatrix} + \begin{Bmatrix} \underline{\mathbf{F}}_{in}(\underline{\mathbf{q}}_e, \dot{\underline{\mathbf{q}}}_e, \dot{q}_m \underline{\mathbf{z}}_m, \underline{\omega}_r) \\ \underline{\mathbf{C}}_{in}(\underline{\mathbf{q}}_e, \dot{\underline{\mathbf{q}}}_e, \dot{q}_m \underline{\mathbf{z}}_m, \underline{\omega}_r) \\ \underline{\mathbf{Q}}_{in}(\underline{\mathbf{q}}_e, \dot{\underline{\mathbf{q}}}_e, \dot{q}_m \underline{\mathbf{z}}_m, \underline{\omega}_r) \end{Bmatrix} + \begin{Bmatrix} \underline{\mathbf{0}} \\ \underline{\mathbf{0}} \\ \underline{\mathbf{k}}_{ee} \cdot \underline{\mathbf{q}}_e \end{Bmatrix} + \begin{Bmatrix} \underline{\mathbf{F}}_g \\ \underline{\mathbf{C}}_g \\ \underline{\mathbf{Q}}_g \end{Bmatrix} = \begin{Bmatrix} \Delta\underline{\mathbf{F}}_c \\ \Delta\underline{\mathbf{C}}_c \\ \Delta\underline{\mathbf{Q}}_c \end{Bmatrix}$$

$$\begin{aligned} \underline{\mathbf{D}}_{rj+1} = \underline{\mathbf{D}}_{rj} &+ \sum_{k=1}^{N_j} \begin{Bmatrix} \underline{\Phi}_{dj,k}(A_{0j+1}) \\ \underline{\Phi}_{rj,k}(A_{0j+1}) \end{Bmatrix} \dot{q}_{ej,k} \\ &- \sum_{k=1}^{N_{j+1}} \begin{Bmatrix} \underline{\Phi}_{dj+1,k}(A_{0j+1}) \\ \underline{\Phi}_{rj+1,k}(A_{0j+1}) \end{Bmatrix} \dot{q}_{ej+1,k} \\ &+ \begin{Bmatrix} \underline{\omega}_{rj} \times \underline{\mathbf{r}}_j(A_{j+1}) \\ \underline{\mathbf{0}} \end{Bmatrix} - \begin{Bmatrix} \underline{\omega}_{rj+1} \times \underline{\mathbf{r}}_{j+1}(A_{j+1}) \\ \underline{\mathbf{0}} \end{Bmatrix} \\ &+ \begin{Bmatrix} \sigma_{j+1}\underline{\mathbf{z}}_{j+1} \\ \bar{\sigma}_{j+1}\underline{\mathbf{z}}_{j+1} \end{Bmatrix} \dot{q}_{rj+1} \end{aligned}$$

where σ_j is a Boolean variable such that $\sigma_j = 1$ if the j^{th} joint is prismatic, 0 if it is rotational and $\bar{\sigma}_j$ is the complementary Boolean variable; $\underline{\mathbf{z}}_j$ is a vector along the j^{th} joint axis and q_{rj} is the j^{th} Lagrangian joint variable.

In the same way two consecutive links of the chain can be isolated to derive the joint equilibrium equation. The generalized force τ_{j+1} acting onto joint A_{j+1} can be written as (Sciavicco and Siciliano, 2000)

$$\begin{aligned} \tau_{j+1} = \underline{\Lambda} \cdot \underline{\mathbf{z}}_{j+1} &+ k_{r_{j+1}} I_{m_{j+1}} \dot{\underline{\omega}}_{rj} \cdot \underline{\mathbf{z}}_{m_{j+1}} \\ &+ k_{r_{j+1}}^2 I_{m_{j+1}} \ddot{q}_{m_{j+1}} \\ &+ k_{r_{j+1}} I_{m_{j+1}} \sum_{k=1}^{N} \underline{\Phi}_{rj,k}(A_{0j+1}) \ddot{q}_{ek_j} \cdot \underline{\mathbf{z}}_{m_{j+1}} \\ &+ k_{r_{j+1}} I_{m_{j+1}} \left(\underline{\omega}_{rj} \times \sum_{k=1}^{N} \underline{\Phi}_{rj,k}(A_{0j+1}) \dot{q}_{ek_j} \right) \cdot \underline{\mathbf{z}}_{m_{j+1}} \end{aligned}$$

where $\underline{\Lambda} = \underline{\mu}_{j+1}$ if A_{j+1} is a rotational joint and $\underline{\Lambda} = \underline{f}_{j+1}$ if A_{j+1} is a prismatic joint, and $\underline{f}_{j+1}$, $\underline{\mu}_{j+1}$ are respectively the force and torque that link S_j exerts onto link S_{j+1}.

Finally, to complete the model, the boundary conditions which occur at both ends of the chain have to be defined.
In the case of an open chain, it seems natural to choose, as shape functions, the cantilever modes of each link. The cantilever modes of the link S_j are embedded in A_j and free in A_{j+1}.
This leads one to impose

$$\underline{\Phi}_{dj,k}(A_j) = \underline{\Phi}_{rj,k}(A_j) = \underline{\mathbf{0}}$$
$$\forall k = 1, \ldots, N_j \qquad \forall j = 1, \ldots, n$$

Furthermore, it is natural to merge the reference points with the A_j's

$$A_j = O_{oj}$$

3. SIMULATION RESULTS

In this section simulation results will be presented, with the particular aim of enucleating the contribution of motors to the dynamic behaviour of the flexible manipulator. The complete model of a flexible manipulator with motors has been derived in a newly conceived environment, FLEXROB, that has been developed under *Maple* 6©. Given the physical and geometrical parameters of the manipulator, FLEXROB produces an optimized model, in the form of an S-function ready to be integrated in *Simulink*©. The complete model will be compared with a simplified one, in which motors are modelled as simple rotating inertias, neglecting gyroscopic effects. This simplified model is obtained under the assumption that the kinetic energy of each rotor is due mainly to its own rotation or, equivalently, that the motion of the rotor is a pure rotation with respect to an inertial frame.
Notice that this approximation is commonly adopted in the rigid robotics (Spong, 1987) and corresponds to the addition of a diagonal matrix, that includes the rotor inertias, to the inertia matrix of the manipulator. The point here is whether with the flexibility and the reduced masses and inertias of the links the approximation is still reasonable.
The prototype considered is a planar manipulator composed of two flexible aluminium links with rectangular section (see Table 1). The strain of each link is described using two modal variables.

Table 1. Prototype specifications

Links	aluminium beam, rectangular section, $0.4m$ length, $0.04m$ height and $0.005m$ width
Base Motor	$4.52Kg$ mass including gear box, rotor inertia $8 \cdot 10^{-6}\ Kg\,m^2$, stator inertia $3.06 \cdot 10^{-4}\ Kg\,m^2$, transmission ratio 200
Elbow Motor	$0.94Kg$ mass including gear box, rotor inertia $2.35 \cdot 10^{-6}\ Kg\ m^2$, stator inertia $1.27 \cdot 10^{-4}\ Kg\ m^2$, transmission ratio 100

The performance of the two models is compared using both a frequency domain analysis and a time domain analysis as in (Stanway *et al.*, 1998).

3.1 *Frequency domain analysis*

The exact values of the unconstrained natural frequencies (Table 2) are evaluated solving the global eigenproblem for the linearized manipulator model:

$$-\omega_\alpha^2 \mathbf{M}(\bar{\mathbf{q}})\mathbf{q}_\alpha + \mathbf{K}(\bar{\mathbf{q}})\mathbf{q}_\alpha = \mathbf{0}, \qquad \alpha = 1, 2, 3, \ldots$$

where ω_α are the natural frequencies, $\mathbf{q}_\alpha$ are the mode shapes and $\bar{\mathbf{q}}$ is the reference configuration, while $\mathbf{M}(\mathbf{q})$ and $\mathbf{K}(\mathbf{q})$ are respectively the global inertia matrix and the stiffness matrix. As can be seen from Table 2, the two models shown differences from about 2% to 60%.

Moreover, recalling that the natural frequencies of a

Table 2. Unconstrained natural frequencies [Hz]

Frequency source	Mode 1	Mode 2	Mode 3	Mode 4
Complete model	6.77	32.44	114.87	176.40
Approx. model	10.77	44.87	116.96	240.71
Error (%)	59.07	38.34	1.82	36.45

bar of length L in bending vibration depend on the mass m as follows (Meirovitch, 1967)

$$\omega_\alpha = (\alpha\pi)^2\sqrt{\frac{EI}{mL^4}}$$

it is evident that taking into account motors yields a decreasing of vibrational frequencies, since the motor masses increase the mass of the link.

3.2 *Time domain analysis*

The time domain analysis is performed using two different kinds of joint space test trajectories. The first one represents a generic "pick-and-place" maneuver (PP) and is characterized by a smooth fifth order polynomial in joint space. This maneuver is a common trajectory used by industrial robots and is also used as a realistic test with flexible manipulators as described in (Zaki and Maraghy, 1992) and (Swevers *et al.*, 1992).
The desired joint trajectory is given by:

$$\theta_d(t) = (\theta_f - \theta_o)\frac{t^3}{T^3}\left[10 - 15\frac{t}{T} + 6\frac{t^2}{T^2}\right]$$

where $\theta_o = \theta_d(0)$ is the initial angle, $\theta_f = \theta_d(T)$ is the desired final angle and T is the duration of the maneuver.
The second maneuver is characterized by a step acceleration (ST) and is designed to excite significant vibrations in the manipulator:

$$\ddot{\theta}_d(t) = \begin{cases} A & 0 < t \le \frac{T}{2} \\ -A & \frac{T}{2} < t \le T \\ 0 & t > T \end{cases}, \qquad A = 4\frac{\theta_f - \theta_o}{T^2}$$

The validity of the models is proved by measuring the error in the energy balance of the system as discussed in (Stanway *et al.*, 1998). The root mean square values of the percentage energy balance error $e_{E,RMS}$ are summarized in Table 3.
The energy error e_E at any time t_i is given by

$$e_E(t_i) = \frac{E(t_i) - W(t_i)}{|E_{peak}|} \cdot 100\%$$

where $W(t_i)$ is the total work input to the system by actuators up to time t_i, $E(t_i)$ is the total mechanical energy of the system and E_{peak} is the maximum energy reached during a maneuver. The RMS value of the percentage energy drift, $e_{E,RMS}$, is evaluated as

$$e_{E,RMS} = \sqrt{\frac{\sum_{i=1}^{N} e_E(t_i)^2}{N}}$$

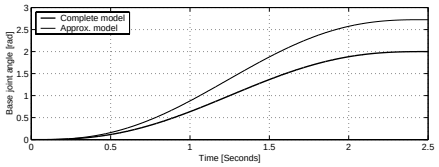

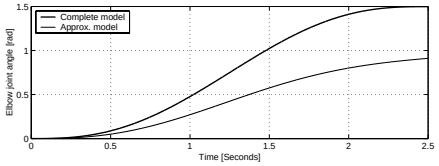

(a) Joint angles

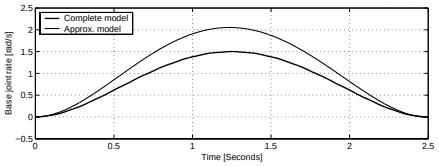

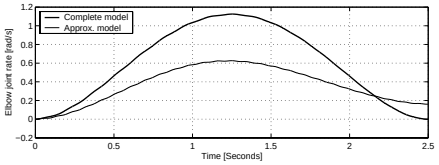

(b) Joint rates

Figure 1. Joint angles and rates for a PP maneuver

where N is the number of discrete time points under consideration.

Table 3. RMS % Energy Drift (25000 points)

Maneuver	Complete model	Approximated model
PP	$2.53 \cdot 10^{-4}$	0.1415
ST	$2.46 \cdot 10^{-3}$	0.1162

Due to lack of space only joint angle trajectories and joint rates for the PP-maneuver (Fig. 1) and link strains for the ST-maneuver (Fig. 2) are presented here.
The PP-maneuver demonstrates the importance of an accurate model of the gyroscopic effects of actuators, in order to avoid steady state errors in joint angles (Fig. 1.a) and over- or under- estimation of the joint rates in the transient behaviour (Fig. 1.b).

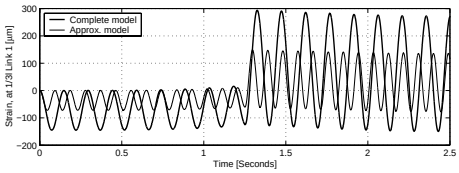

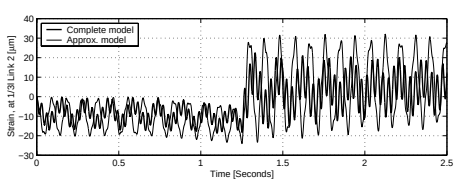

Figure 2. Strains for an ST maneuver

On the other hand the ST-maneuver excites vibrational modes and shows the effects on link strains (Fig. 2) due to the errors, discussed in the frequency domain analysis section, in estimating the natural frequencies.

4. CONCLUSIONS

A model developed for simulation or model based control should be both computationally efficient and as accurate as possible. The model described in this paper matches to some extent both of the above requirements, as it exploits the most efficient methodology known to date to model mechanical chained structures and it accounts in a rigorous way for the actuators at the joints of the chain. Realism can thus be given to simulations without overcomplicating the computation algorithms.
An idea of the efficiency obtained using both recursive algorithm and symbolic simplification can be achieved evaluating the computational load, due to a sequence of operations, with the *Maple*© cost function. Consider, for simplicity, the model of a two link flexible manipulator without motors, developed using Eulero-Lagrange equations and the FLEXROB package. The load of the first model is 1899 trigonometric function calls, 1497 additions and 7418 multiplications. On the other hand, the model obtained using FLEXROB has a load of 2 trigonometric function calls, 484 additions, 648 multiplications and 3 divisions.

Experimental validation of the model is being currently performed on a prototype laboratory test bed.

5. REFERENCES

Book, W.J. (1984). Recursive lagrangian dynamics of flexible manipulator arms. *International Journal of Robotics Research* **3**(3), 87–101.

Boyer, F. and P. Coiffet (1996). Generalization of newton-euler model for flexible manipulators. *Journal of Robotic Systems* **13**(1), 11–24.

Cetinkunt, S. and W.J. Book (1987). Symbolic modelling of flexible manipulators. *IEEE international conference on Robotics Automation* pp. 2074–2080.

Hughes, P.C. and G.B. Sincarsin (1989). Dynamics of elastic multibody chains: Part a - body motion equations. *Journal of Dynamic Stability Systems* **4**(3 and 4), 209–226.

Kane, T.R. and D.A. Levinson (1980). Formulation of equations of motion for complex spacecraft. *Journal of Guidance and control* **3**(2), 99–112.

Kane, T.R., R.R. Ryan and A.K. Banerjee (1987). Dynamic of a cantilever beam attached to a moving base. *Journal of Guidance, Control and Dynamics* **10**(2), 139–151.

Meirovitch, L. (1967). *Analytical methods in vibrations*. Macmillan Publishing.

Padilla, C.E. and A.H. Von Flottow (1992). Nonlinear strain-displacement relations and flexible multibody dynamics. *Journal of Guidance, Control and Dynamics* **15**(1), 128–136.

Sciavicco, L. and B. Siciliano (2000). *Modeling and control of robot manipulators*. 2nd ed.. Springer-Verlag.

Singh, R.P., V. Voort and R.J. Likins (1984). Dynamics of flexible bodies in tree topology - a computer oriented approach. *Proceedings of the AIAA Dynamics specialist conference* pp. 327–337.

Spong, M.W. (1987). Modeling and control of elastic joint robots. *Journal of Dynamic Systems, Measurement and Control* **109**, 310–319.

Stanway, J., I. Sharf and C. Damaren (1998). Comparison and validation of dynamics simulation models for a structurally flexible manipulator. *Transactions of the ASME* **120**, 404–409.

Swevers, J., D. Torfs, F. Demeester and H. Van Brussel (1992). Fast and accurate tracking control of a flexible one-link robot based on real-time link deformation measurements. *Mechatronics* **2**(1), 29–41.

Zaki, A.S. and W.H. El Maraghy (1992). Modeling and control of a two-link flexible manipulator. *Transactions of the CSME* **16**(3/4), 311–328.